Available online at www.sciencedirect.com
SCIENCE DIRECT
ACADEMIC PRESS
Journal of Sound and Vibration 268 (2003) 799–808
JOURNAL OF SOUND AND VIBRATION
www.elsevier.com/locate/jsvi

Application of magnetomechanical sensors for modal testing

Yoon Young Kim*, Seung Hyun Cho, Ho Cheol Lee

School of Mechanical and Aerospace Engineering and National Creative Research Initiatives Center for Multiscale Design, Seoul National University, San 56-1, Shilim-dong, Kwanak-gu, Seoul 151-742, South Korea

Received 6 July 2001; accepted 20 November 2002

Abstract

A new modal testing technique using magnetomechanical sensors is proposed in this paper. To list some advantages of this technique, sensors are cost-effective and require no direct physical contact with a structure. The specific application made in this paper is the modal testing for the bending vibration of a solid circular beam. The theoretical analysis explaining the principle of the magnetostrictive sensor-based modal testing is presented for beam bending. The present results are compared with those obtained by the use of standard accelerometers. Although the application of this technique is made to relatively simple problems, the potential of magnetomechanical sensors for modal testing has been revealed.

1. Introduction

Modal testing is one of the most important procedures for dynamic system identification [1]. In modal testing, accelerometers or strain gauges are popular sensors, but they require the physical contact with structures to be tested. For non-contact sensing of vibration signals, laser-based measurement techniques may be applied. Although the laser-based techniques have been succesful in many applications, the sensing system is quite expensive. In an attempt to develop a cost-effective non-contact modal testing scheme, we propose to employ magnetomechanical sensors for vibration signal measurements. The main part of the sensors simply consists of inexpensive coils and bias magnets.

The principle of magnetomechanical sensors is based on the Villari effect [2]. This effect represents the phenomenon of the magnetic flux change of ferromagnetic materials when they are subjected to mechanical stress. These sensors were applied for the construction of delay lines of

*Corresponding author. Tel.: +82-2-880-7154; fax: +82-2-883-1513.
E-mail addresses: yykim@snu.ac.kr (Y.Y. Kim), ploydin@idealab.snu.ac.kr (S.H. Cho), hclee@idealab.snu.ac.kr (H.C. Lee).

0022-460X/03/$ - see front matter
doi:10.1016/S0022-460X(03)00476-0

electric signals [3]. The most successful applications of the sensors in mechanical systems are the measurements of (ultrasonic) elastic waves [4–8]. The typical frequency range considered lies between a few kHz and 300 kHz, but there has been no attempt to use the sensors in modal testing where relatively low-frequency (below 10 kHz) vibration responses are of a major concern. Furthermore, there is no theoretical analysis justifying the use of the magnetomechanical sensors for modal analysis.

The goal of this paper is to develop a modal testing method based on magnetomechanical sensors and to present a simplified theoretical analysis justifying the feasibility of the magnetomechanical sensor-based modal testing method. The specific application in this work is made in the modal testing of bending vibrations of a freely supported beam made of steel. The first lowest eigenfrequency considered is in the order of 10^2 Hz. For the modal testing, the beam structure is excited by an impact hammer. The eigenfrequencies and bending mode shapes determined from the present method are compared with those obtained by the use of typical accelerometers. Although the present application is rather limited to simple beam problems, the present method may be extended to other types of structures such as plate and shell structures.

2. Modelling of magnetomechanical effects in a rod under bending

When a piece of ferromagnetic materials is placed in a time-varying magnetic field, its physical dimension varies. This effect is known as the magnetostriction effect or the Joule effect [9]. Joule has showed that the length of an iron rod increases or decreases when it is magnetized in the longitudinal direction.

When a piece of ferromagnetic material under a magnetic field is subjected to a change of a stress field, it exhibits the change in the amount of the magnetization. This reverse phenomenon is usually referred to as the inverse magnetostriction effect or the magnetomechanical effect [10,11]. In particular, the longitudinal inverse magnetostriction effect is called the Villari effect [12]. For small reversible changes in stress, the following relation [13] holds:

$$\left.\frac{\partial \varepsilon}{\partial H}\right)_{\sigma} = \left.\frac{\partial B}{\partial \sigma}\right)_{H},$$

where B and H denote the magnetic flux density and the magnetic field strength, respectively. The strain and stress of the material are expressed by ε and σ, respectively. Recently, Jiles [11] has proposed a theory explaining the magnetomechanical effect in which hysteresis and irreversibility are considered.

At the crystalline level, magnetostrictive materials contain many magnetic domains that have the same direction of the atomic moment. The applied stress to the materials changes the directions of magnetic domains (see Fig. 1). When a coil encircles a part of a rod made of magnetostrictive materials, the change of the magnetic flux density caused by elastic waves propagating in the bar can be converted to the voltage potential output of the coil. In this case, the coil serves as the main element of a sensor, which is usually referred to as a magnetomechanical sensor.

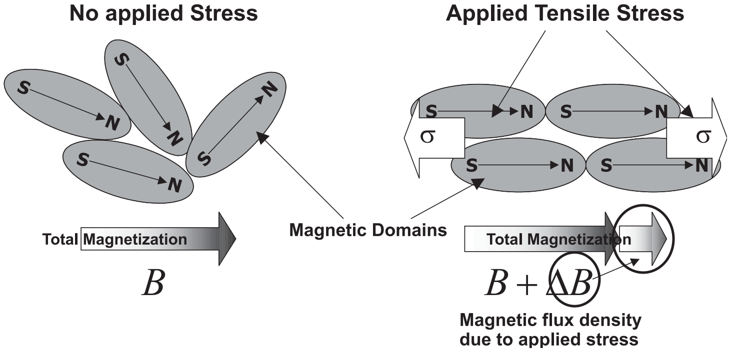

Fig. 1. The schematic description of the magnetostriction effects.

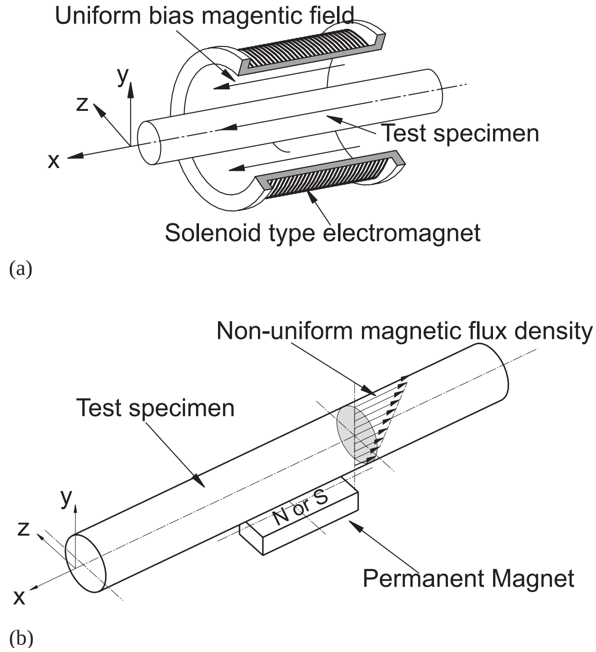

Fig. 2. Typical distributions of the bias magnetic field applied to a beam: (a) uniform field, and (b) non-uniform field.

Since our work is mainly concerned with the use of magnetomechanical sensors in a slender beam, the following linearized model [14,15] may be considered:

$$B = B_H + B_\sigma \tag{1}$$

and

$$B_H = \mu^\sigma H, \tag{2}$$

$$B_\sigma = q\sigma. \tag{3}$$

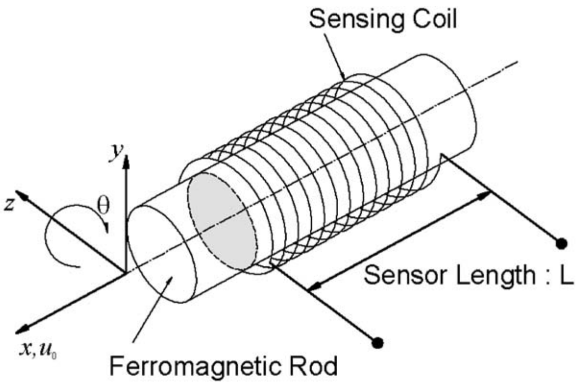

Fig. 3. The schematic diagram of a turn of a coil around a circular beam with a coordinate system shown.

In Eq. (2), μ^σ is the permeability for a constant stress and q represents the magnetoelastic coupling coefficient. Here, B and H represent the components in the direction of the beam axis.

When the applied magnetic field in a beam is uniform across its cross-section as shown in Fig. 2(a), the magnetoelastic coupling coeffecient q can be assumed to be constant along the y-axis. However, q cannot be assumed to be constant when a non-uniform magnetic field is applied as shown in Fig. 2(b).

When a beam is slender and bends in the xy plane (see Fig. 3), the distribution of the bending stress may be assumed to be linear in y. Since bending in the xz plane is not considered, B_H and B_σ may be assumed to be independent of z:

$$B_H = B_H(x, y) = \mu^\sigma H(x, y), \tag{4}$$

$$B_\sigma = B_\sigma(x, y, t) = q(B_H(x, y))\sigma(x, y, t). \tag{5}$$

The magnetic flux density B_H results from a static magnetic field strength H. Unless $H(x, y)$ is uniform across the beam cross-section, the variation of B_σ in the y-axis must be taken into account.

3. Modal analysis using a magnetomechanical sensor

Based on the discussions given in Section 2, an experimental setup shown in Fig. 4 is prepared. A permanent magnet is used to magnetize the area of the beam encircled by a magnetomechanical sensor. Although an optimal distribution of the magnetic field strength may be found, we here choose the simplest magnet arrangement for bending vibration measurements, which is shown in Fig. 4. (Similar magnet configurations have been used in earlier investigations of wave dispersions [4,5].)

In this section, we will present an analysis to justify the usefulness of magnetomechanical sensors for modal testing. Neglecting non-linearity and hysteresis, the magnetoelastic coupling coeffecient q in Eq. (5) may be expanded as

$$q(x, y) = c_0(x) + c_1(x)y + c_2(x)y^2 + \cdots. \tag{6}$$

This approximation can be useful in the analysis of bending vibrations in a slender beam.

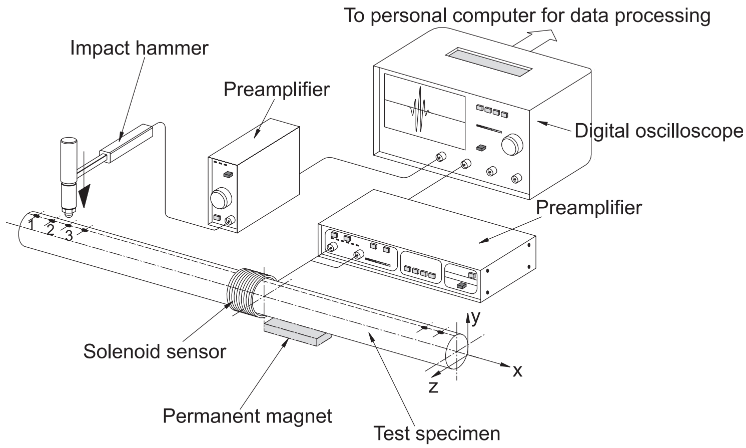

Fig. 4. The schematic diagram of the experimental arrangement for a circular steel beam (length $=916$ mm, and diameter $=25$ mm).

The longitudinal displacement $u_x(x, y, t)$ predicted by a beam theory is given by (see, e.g., Ref. [16])

$$u_x(x, y, t) = u_0(x, t) - y\theta\ (x, t), \tag{7}$$

where u_0 and θ denote the average displacement across the beam cross-section and the rotation of a normal about the z-axis. (See Fig. 3 for the definition of the positive directions.)

The resulting stress σ due to the displacement u_x is written as

$$\sigma_x = E\frac{\partial u_x}{\partial x} = E\left(\frac{\partial u_0}{\partial x} - y\frac{\partial \theta}{\partial x}\right), \tag{8}$$

where E is Young's modulus. When the bending strain (thus stress) is dominant inside the beam, Eq. (8) can be simplified to

$$\sigma_x(x, y, t) = -Ey\frac{\partial \theta(x, t)}{\partial x}. \tag{9}$$

Substituting Eqs. (6) and (9) into Eqs. (1)–(3) yields

$$B(x, y, t) = -E(c_0(x)y + c_1(x)y^2 + \cdots)\frac{\partial \theta}{\partial x} + \mu^\sigma H(x, y). \tag{10}$$

The magnetic flux $\phi(x, t)$ passing through a turn of the coil is given by (in case of n turns, the following result is multiplied by n):

$$\begin{aligned}\phi(x, t) &= \int_A B\,\mathrm{d}A \\ &= -E\frac{\partial \theta}{\partial x}\left[c_0(x)\int_A y\,\mathrm{d}A + c_1(x)\int_A y^2\,\mathrm{d}A + \cdots\right] + \int_A \mu^\sigma H(x, y)\,\mathrm{d}A,\end{aligned} \tag{11}$$

where A is the cross-sectional area of the beam. For a circular cross-section,

$$\int_A y\,\mathrm{d}A = 0, \quad \int_A y^2\,\mathrm{d}A \equiv I, \tag{12}$$

where I is the moment of inertia about the z-axis of the beam cross-section. Since μ^σ and $H(x, y)$ in Eq. (11) are time independent, the output voltage $v(x, t)$ measured by the coil at location x is given by

$$v(x,t) = -\frac{\partial \phi}{\partial t} = EIc_1(x)\frac{\partial^2 \theta}{\partial t \partial x} + (higher\ order\ terms). \tag{13}$$

Since the bending moment $M(x, t)$ is approximated by

$$M = EI\frac{\partial \theta}{\partial x}, \tag{14}$$

Eq. (13) reduces to

$$v(x,t) = c_1(x)\frac{\partial M(x,t)}{\partial t} + (higher\ order\ terms). \tag{15}$$

Eq. (15) states that the measured voltage output through the coil is equivalent to the time derivative of the bending moment of the beam. It is clear from Eq. (15) that the presence of $c_1(x)$, i.e., the linear bias field, must be ensured for bending vibration measurement. Furthermore, the present analysis is valid for slender beams.

For a given harmonic excitation force $f(x, t)$

$$f(x,t) = F(x)\,\mathrm{e}^{\mathrm{i}\omega t}, \tag{16}$$

the steady state forced-vibration responses may be written as [16]

$$w(x,t) = W(x)\,\mathrm{e}^{\mathrm{i}\omega t} = \sum_{r=1}^{\infty} C_r(\omega)W^{(r)}\,\mathrm{e}^{\mathrm{i}\omega t}, \tag{17}$$

$$\theta(x,t) = \Theta(x)\,\mathrm{e}^{\mathrm{i}\omega t} = \sum_{r=1}^{\infty} C_r(\omega)\,\Theta^{(r)}\,\mathrm{e}^{\mathrm{i}\omega t}, \tag{18}$$

$$M(x,t) = N(x)\,\mathrm{e}^{\mathrm{i}\omega t} = \sum_{r=1}^{\infty} C_r(\omega)N^{(r)}\,\mathrm{e}^{\mathrm{i}\omega t}, \tag{19}$$

where $W^{(r)}, \Theta^{(r)}$, and $N^{(r)}$ are the rth mode shapes of the transverse displacement, the rotation of the normal, and the moment. The unknown coefficient $C_r(\omega)$ can be found from the orthogonality condition [18],

$$\int_0^L \rho A[W^{(r)}(x)W^{(s)}(x) + r_g^2\,\Theta^{(r)}(x)\,\Theta^{(s)}(x)]\,\mathrm{d}x = \delta_{rs}, \tag{20}$$

where L is the beam length and ρ is the mass density of the beam.

The resulting expression for $N(x)$ is

$$N(x) = \sum_{r=1}^{\infty}\frac{N^{(r)}(x)}{\Omega_r^2 - \omega^2}\int_0^L W^{(r)}(x)F(x)\,\mathrm{d}x, \tag{21}$$

where Ω_r is the rth eigenfrequency. If $F(x)$ is a point force applied at $x = x_j$ as

$$F(x) = F_j\delta(x - x_j), \tag{22}$$

the frequency response of the bending moment at $x = x_i$ is given by γ_{ij},

$$\gamma_{ij} \equiv \frac{N(x_i)}{F_j} = \sum_{r=1}^{\infty} \frac{N_i^{(r)} W_j^{(r)}}{\Omega_r^2 - \omega^2}, \tag{23}$$

where $N_i^{(r)} = N^{(r)}(x_i)$, and $W_j^{(r)} = W^{(r)}(x_j)$.

If the voltage output $v(x,t)$ is put into the following form:

$$v(x,t) = V(x)\,\mathrm{e}^{\mathrm{i}\omega t}, \tag{24}$$

and Eq. (15) is used, the frequency response ξ_{ij} of the measured voltage output can be finally written as

$$\xi_{ij} \equiv \frac{V(x_i)}{F_j} = c_1(x_i) \sum_{r=1}^{\infty} \frac{\mathrm{i}\omega N_i^{(r)} W_j^{(r)}}{\Omega_r^2 - \omega^2}. \tag{25}$$

From Eq. (25), it is clear that the bending mode shape $N^{(r)}$ can be determined if the measurement locations vary while the excitation location is fixed. On the other hand, if the excitation location varies with the measurement location fixed, the displacement mode shape $W^{(r)}$ can be determined. Since typical modal analysis requires the displacement mode shape $W^{(r)}$, we will consider only the determination of $W^{(r)}$. The present mode shapes determined by the use of a magnetomechanical sensor will be compared with those obtained by the use of an accelerometer.

4. Experimental results

Fig. 4 shows a schematic diagram of the present experimental arrangement. For the verification of the present modal testing technique, a freely supported beam is considered. In actual experiments, the beam is suspended at its ends by elastic cords having very low stiffness. A coil-type magnetomechancial sensor has been prepared. The length and the inside diameter of the coil are 9 and 33 mm, respectively. The coil has 150 turns made of 0.3 mm thick wires.

The center of the magnetomechanical sensor is placed 412 mm away from an end. After the bias magnet has been placed at one side of the coil for the magnetization of a part of the beam (see Fig. 2(b)), it is removed in order not to bend the beam during the measurement.

To determine the displacement mode shape $W^{(r)}$, the impact point locations are changed while the sensor location remains unchanged. More specifically, the beam is excited at 29 locations which are uniformly spaced with the distance of 30.5 mm.

The impact hammer signal is amplified by the PCB 432A16 amplifier and the detected signal at the sensor is amplified by the SR560 low-noise amplifier. The amplified signal is then digitized in the LeCroy 9310M oscilloscope.

For the present verification, two experiments are conducted. Case 1 corresponds to an experiment without applying the bias magnetic field. Case 2 corresponds to the experiment on a beam whose sensing part has been magnetized by a permanent magnet. In the present experiment, the flux density near the pole surface of the magnet is only 0.33 T.

The magnetization level will affect the sensor output, but it may be treated as a calibration constant. When mode shapes and eigenfrequencies are of a main concern, the exact calibration constant does not need to be determined. However, the effects of the magnetization level and the material hysteresis on the sensor output have been investigated by Lee [17]. It is also remarked that a few percent demagnetization in typical ferromagnetic materials usually requires several days or longer, so the magnetization level remains virtually unaltered during modal testing.

The experimental results obtained by the two cases are compared with those obtained by a conventional modal testing method based on an accelerometer. Fig. 5 shows the frequency response function for the excitation made at point 1 obtained by the present technique. The results corresponding to Cases 1 and 2 are shown in Figs. 5(a) and 5(b), respectively. When no bias field is applied, the resulting frequency response function (FRF) is not as good as the one obtained with pre-magnetization, but it is still reasonable. The same behavior is observed for FRFs at all other locations. However, the comparison of these two figures demonstrates the role of the bias magnetic field, which has also been discussed in similar applications [4].

The eigenfrequencies obtained by the present magnetomechanical sensor-based method are compared in Table 1 with those by the modal testing method using an accelerometer. The two

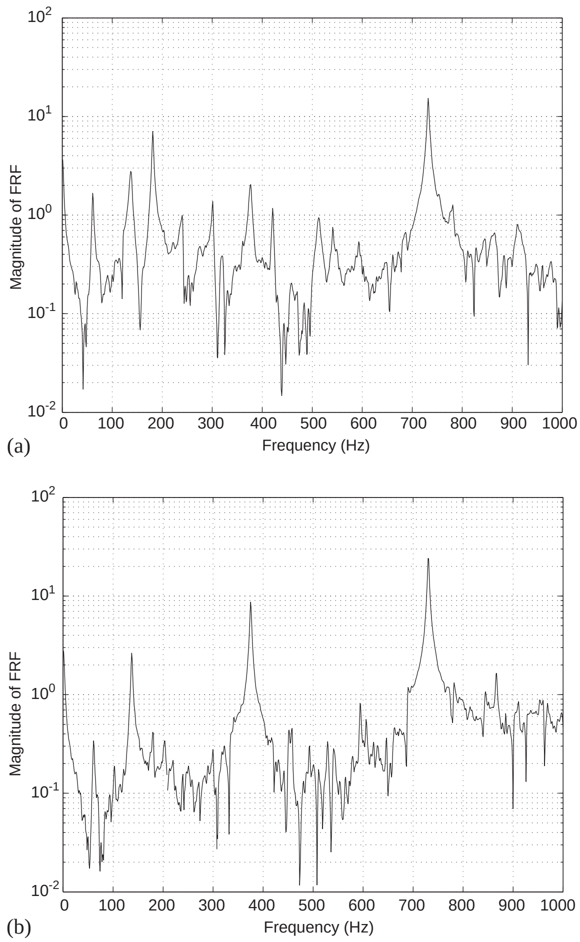

Fig. 5. The frequency response functions (FRFs) of a free–free beam shown in Fig. 4 for (a) case 1 (without pre-magnetization and (b) case 2 (with pre-magnetization).

Table 1
Eigenfrequencies of the beam shown in Fig. 4 (unit: Hz, resolution 0.1 Hz)

Mode number	1	2	3	4
Accelerometer	136.1	374.1	729.1	1197.9
Magnetomechanical sensor	136.1	374.2	729.5	1198.3

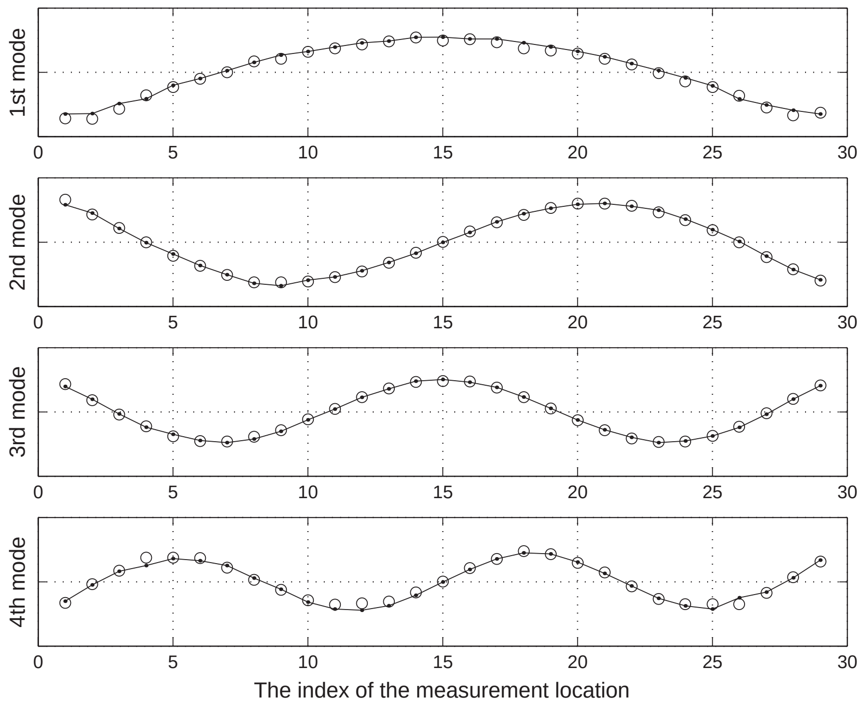

Fig. 6. The displacement mode shapes $W^{(r)}$ of a free–free beam shown in Fig. 4 (solid lines: by an accelerometer; circles: the present result by a magnetostrictive sensor).

values are virtually indistinguishable. The lowest first four vibration mode shapes are also compared in Fig. 6.

5. Conclusions

Magnetomechanical sensors are suggested as non-contact, cost-effective sensors for modal testing. The theory of the magnetomechanical sensor-based modal testing was presented for the bending vibration measurement of a beam. The experimental results obtained for a beam confirmed the validity and the effectiveness of the present method. Although the present application was made in a relatively simple problem, the present work suggests the possibility of the application of the magnetostrictive sensors for modal testing of more complex structures made of ferromagnetic materials.

References

[1] D.J. Ewins, Modal Testing: Theory and Practice, Research Studies Press, Letchworth, 1984.
[2] E. Villari, Change of magnetization by tension and by electric current, Annalen der Physik und Chemie, Leipzig 126 (1865) 87–122.
[3] R.C. Williams, Theory of magnetostrictive delay lines for pulse and continuous wave transmission, IEEE Transactions on Ultrasonic Engineering UE-7 (1959) 16–38.
[4] H. Kwun, C.M. Teller, Magnetostrictive generation and detection of longitudinal, torsional, and flexural waves in a steel rod, Journal of the Acoustical Society of America 96 (2) (1994) 1202–1204.
[5] H. Kwun, K.A. Bartels, Experimental observation of wave dispersion in cylindrical shells via time-frequency analysis, Journal of the Acoustical Society of America 97 (6) (1995) 3905–3907.
[6] H. Kwun, K.A. Bartels, Experimental obsevation of elastic-wave dispersion in bounded solids of various configurations, Journal of the Acoustical Society of America 99 (2) (1996) 962–968.
[7] H. Kwun, K.A. Bartels, Magnetostrictive sensor technology and its applications, Ultrasonics 36 (1998) 171–178.
[8] H.C. Lee, Y.Y. Kim, Wave selection using a magnetomechanical sensor in a solid cylinder, Journal of the Acoustical Society of America 112 (3) (2002) 953–960.
[9] B.D. Cullity, Introduction to Magnetic Materials, Addison-Wesley, Reading, MA, 1972.
[10] B. Jones, C. Liang, Magnetostriction: revealing the unknown, IEEE Aerospace and Electronic Systems Magazine (1996) 3–6.
[11] D.C. Jiles, Theory of the magnetomechanical effect, Journal of Physics D: Applied Physics 28 (1995) 1537–1546.
[12] J.B. Restorff, Magnetostrictive Materials and Devices, Encyclopedia of Applied Physics, Vol. 9, VCH Publisher, New York, 1994, pp. 229–244.
[13] R.M. Bozorth, Ferromagnetism, Van Nostrand, New York, 1951.
[14] A.E. Clark, Ferromagnetic Materials, Vol. 1, North-Holland, Amsterdam, 1980.
[15] M.J. Dapino, R.C. Smith, A.B. Flatau, Structural magnetic strain model for magnetostrictive transducers, IEEE Transactions on Magnetics 36 (3) (2000) 545–556.
[16] Y.Y. Kim, J.H. Kang, Strain-based rotational mode measurement in a beam, Journal of Sound and Vibration 222 (2) (1999) 225–237.
[17] H.C. Lee, Design and Analysis of a Mode-selectable Stress Wave Sensor using the Villari Effect, Ph.D. Thesis, Seoul National University, Seoul, Korea, 2001.
[18] T.C. Huang, The effect of rotary inertia and of shear deformation on the frequency and normal mode equations of uniform beams with simple end conditions, Journal of Applied Mechanics 28 (1961) 579–584.